Free Radical Biology and Medicine 90 (2016) 24–34

Contents lists available at ScienceDirect

Free Radical Biology and Medicine

journal homepage: www.elsevier.com/locate/freeradbiomed

Original Contribution

Reversible oxidation of phosphatase and tensin homolog (PTEN) alters its interactions with signaling and regulatory proteins

Ivan Verrastro [a], Karina Tveen-Jensen [a], Rudiger Woscholski [b], Corinne M. Spickett [a], Andrew R. Pitt [a,*]

[a] School of Life and Health Sciences, Aston Triangle, Aston University, Birmingham B4 7ET, UK
[b] Department of Chemistry and Institute of Chemical Biology, Imperial College London, UK

ARTICLE INFO

Article history:
Received 8 May 2015
Received in revised form
4 November 2015
Accepted 5 November 2015
Available online 10 November 2015

Keywords:
Protein oxidation
Mass spectrometry
Proteomics
Protein–protein interactions
Peroxiredoxin-1
Redox biology
Signaling
Thioredoxin-1

ABSTRACT

Phosphatase and tensin homolog (PTEN) is involved in a number of different cellular processes including metabolism, apoptosis, cell proliferation and survival. It is a redox-sensitive dual-specificity protein phosphatase that acts as a tumor suppressor by negatively regulating the PI3K/Akt pathway. While direct evidence of redox regulation of PTEN downstream signaling has been reported, the effect of PTEN redox status on its protein–protein interactions is poorly understood. PTEN-GST in its reduced and a DTT-reversible H_2O_2-oxidized form was immobilized on a glutathione-sepharose support and incubated with cell lysate to capture interacting proteins. Captured proteins were analyzed by LC–MSMS and comparatively quantified using label-free methods. 97 Potential protein interactors were identified, including a significant number that are novel. The abundance of fourteen interactors was found to vary significantly with the redox status of PTEN. Altered binding to PTEN was confirmed by affinity pull-down and Western blotting for Prdx1, Trx, and Anxa2, while DDB1 was validated as a novel interactor with unaltered binding. These results suggest that the redox status of PTEN causes a functional variation in the PTEN interactome. The resin capture method developed had distinct advantages in that the redox status of PTEN could be directly controlled and measured.

© 2015 The Authors. Published by Elsevier Inc. This is an open access article under the CC BY license (http://creativecommons.org/licenses/by/4.0/).

1. Introduction

PTEN is a dual specificity phosphatase that has attracted significant interest from the biomedical research community over the last two decades. The *PTEN* gene is mutated in many cancers and its phosphatase protein product has been implicated as a negative regulator of the PI3K/Akt pathway [1–4]. PTEN dephosphorylates the signaling intermediate PtdIns(3,4,5)P_3 (phosphatidylinositol-3,4,5-bisphosphate) to PtdIns(4,5)P_2 (phosphatidylinositol-4,5-bisphosphate), suppressing the PI3K-dependent signaling cascade that leads to the activation of the intracellular protein Akt (also known as protein kinase B, PKB) [5]. The activation of Akt triggers the signal responsible for the modulation of many cellular functions, including cell cycle regulation, cell growth, apoptosis, angiogenesis, protein synthesis, transcription and proliferation [6–9]. It has been reported that PTEN phosphatase activity is inactivated when treated with oxidizing agents *in vitro*, as well as in cells exposed to oxidative stress conditions [10–12]. Reversible inactivation of PTEN has been shown upon hydrogen peroxide oxidation, which results in the formation of a disulfide bond between Cys71 and Cys124 in the N-terminal phosphatase domain of the protein [11]. PTEN protein interactions play an important role in the function of PTEN beyond its simple phosphatase activity [8], and it has been suggested that as well as affecting catalytic activity, this oxidation of PTEN might also modulate its ability to interact with its binding partners, thereby affecting downstream signaling [13]. However, few studies to date have described the

Abbreviations: AKAP12, A-kinase anchor protein 12; ANOVA, analysis of variance; Anxa2, annexin A2; Cys, cysteine; DDB1, DNA damage-binding protein 1; Dreb, drebrin; Dsp, desmoplakin; DTT, dithiothreitol; EDTA, ethylenediaminetetraacetic acid; FAS, fatty acid synthase; GAPDH, glyceraldehyde 3-phosphate dehydrogenase; GSH, glutathione; GST, glutathione S-transferase; GNAI, guanine nucleotide-binding protein G(i); GTPase, guanosine triphosphatase; HCC, hepatocellular carcinoma; HER2, human epidermal growth factor 2; HPLC, high performance liquid chromatography; HRP, horseradish peroxidase; HSPs, heat shock proteins; LC, liquid chromatography; Met, methionine; MPRIP, myosin phosphatase Rho-interacting protein; MS, mass spectrometry; NADPH, Nicotinamide adenine dinucleotide phosphate; Nox, NADPH oxidase; OMFP, 3-*O*-methylfluorescein phosphate; OxPTMs, oxidative post-translational modifications; PI3K, phosphoinositide 3-kinase; PtdIns(4,5)P_2, phosphatidylinositol-4,5-bisphosphate; PtdIns(3,4,5)P_3, phosphatidylinositol-3,4,5-triphosphate; Pelo, protein pelota homolog; PDIP2, polymerase delta-interacting protein 2; Prdx1, peroxiredoxin-1; PKA, protein kinase A; PKC, protein kinase C; PTEN, phosphatase and tensin homolog (deleted on chromosome 10); PTPs, protein tyrosine phosphatases; RT, retention time; SOD, superoxide dismutase; Spta1, spectrin α-chain; Trx, thioredoxin-1

* Corresponding author.
E-mail address: a.r.pitt@aston.ac.uk (A.R. Pitt).

http://dx.doi.org/10.1016/j.freeradbiomed.2015.11.004
0891-5849/© 2015 The Authors. Published by Elsevier Inc. This is an open access article under the CC BY license (http://creativecommons.org/licenses/by/4.0/).

effect of altered redox status on the signaling pathways and protein–protein interactions of PTEN.

Several different techniques have been used to characterize the PTEN interactome over the last two decades, and have produced both high-throughput and low-throughput data [14–17]. Previous research in mammalian cells treated with H_2O_2 has shown increased binding of DJ-1 (also known as Parkinson disease 7, PARK7) to PTEN, reduction in PTEN catalytic activity, and enhanced phosphorylation of Akt [18], resulting in increased cell proliferation and apoptosis. Similarly, the association between thioredoxin (Trx) and PTEN has been shown to be redox-regulated [19]. Trx plays an important role in the re-activation of PTEN *in vivo* after H_2O_2 treatment and has been demonstrated to be even more efficient than glutathione or glutaredoxin in the reduction of oxidized PTEN [10]. The interaction between PTEN and peroxiredoxin-1 (Prdx1) has also been proposed as a possible mechanism to protect PTEN from hydrogen peroxide-induced inactivation, thereby preserving its tumor suppressing function [20]. Generally, these studies suggest that there could be a correlation between cellular redox status and the regulation of specific PTEN protein–protein interactions. This relationship needs to be investigated further, as such mechanisms are likely to be involved in the modulation of tumorigenesis and stress-related cellular processes.

Mass spectrometry (MS) methods used in combination with affinity capture-based experiments are a valuable and well-recognized tool to investigate protein–protein interactions [21]. Along with data providing evidence of protein identity, accurate information on protein abundance is also required to generate high-throughput protein–protein interaction datasets. Methodologies based on *in vivo* isotope labeling are a common choice for absolute and relative quantification of protein–protein interaction data [22] and offer the advantage of minimal errors in the final quantification, but present a number of significant limitations, including amenability of certain cell lines to grow in modified media, labeling-induced artifacts, and limited availability of required reagents [23]. Recently, label-free methods have become more popular in the field of LC–MS-based interactomics [24]. These do not require additional sample manipulation steps, and represent a fast, straightforward, and relatively cost-effective method to perform comparative analysis between different protein mixtures in complex biological samples. New generation label-free *in silico* solutions rely on accurate feature intensity-based quantification and are capable of processing large amount of high resolution data [25]. Over the past few years, complex proteome-wide data such as those generated from biomarker discovery and protein–protein interactions studies, have been analyzed by proteomics researchers using label-free quantification, with accurate and reliable results [26].

We hypothesized that oxidative-induced inactivation of PTEN would modulate the ability of the protein to bind its interacting partners, thus altering its interactome. To investigate this, a GST-tagged fusion PTEN was immobilized on a glutathione-sepharose resin and challenged with HCT116 cell lysate for the affinity-capture of the interactions. Using label-free quantitative LC–MS/MS, we compared the abundance of the binding proteins between reduced and oxidized PTEN. In addition, the method described identified a number of putative novel protein–protein interactions that contribute to shedding a light on the possible involvement of PTEN in several cellular processes of current interest.

2. Materials and methods

2.1. Reagents

All reagents were purchased from Fisher Scientific (Loughborough, UK), unless otherwise indicated. All solvents were of LC–MS grade and Milli-Q water was used at all times. Monoclonal antibodies against Trx (ab16965) and Anxa2 (ab54771) were purchased from Abcam (Cambridge, UK). Monoclonal antibodies against Prdx1 (D5G12), DDB1 (D4C8) and PTEN (26H9) were purchased from Cell Signaling Technology. HRP-linked anti-mouse IgG secondary antibody was purchased from Santa-Cruz (sc-2031) and HRP-linked anti-rabbit IgG was from Cell Signaling Technology (7074S). Enhanced chemiluminescence (ECL kit) was from Pierce, Life Technologies, Paisley, UK. Reduced L-glutathione, methionine, 3-*O*-methylfluorescein phosphate (OMFP) cyclohexylammonium salt, bovine serum albumin (BSA), bromophenol blue and SDS-PAGE Sample Buffer Laemmli 2 × concentrate were supplied by Sigma-Aldrich Chemical Co., Dorset, UK. 3-*O*-methylfluorescein (OMF) was obtained from Apollo Scientific, Denton, UK.

2.2. Expression and purification of PTEN

Glutathione S-transferase (GST)-PTEN cDNA was cloned into the PGEX-4T1 plasmid. *Escherichia coli* DH5α calcium chloride-competent cells (100 μL) were transformed with 1 μL of 47.6 ng/μL PGEX-4T1-PTEN-GST expression plasmid DNA by incubating on ice for 30 min, heat shocking at 42 °C for 90 s, followed by another incubation on ice for 2 min. The transformed cells were then incubated at 37 °C for 1 h in a shaking incubator (Infors AG, Bottmingen, Switzerland) at 180 rpm, and plated onto sterile LB-agar containing 100 μg/mL ampicillin sodium salt (Sigma-Aldrich Chemical Co., Dorset, UK). Following incubation overnight at 37 °C, isolated bacterial colonies were picked from the plate and pre-cultured in 10 mL of LB Broth medium supplemented with 100 μg/mL ampicillin at 180 rpm for 16 h at 37 °C. Cultures were grown in 1 L LB Broth supplemented with 100 μg/mL ampicillin at 37 °C and at 180 rpm in a shaking incubator (MAXQ 8000, Thermo Scientific, Hemel Hemstead, UK) until the optical density at 600 nm (OD_{600}) reached 0.5–0.6, at which point isopropyl-β-D-1-thiogalactopyranoside (IPTG) was added to a final concentration of 1 mM to induce protein expression, and the cultures grown for a further 24 h at 23 °C.

The cells were harvested by centrifugation at 4645*g* for 20 min at 4 °C. Pellets were resuspended in 50 mM Tris pH 7.4 supplemented with EDTA-free protease inhibitor cocktail (Catalog no. 11 873 580 001, Roche Diagnostics GmbH, Mannheim, Germany), the suspension was centrifuged at 4800*g* for 20 min at 4 °C, the supernatant removed and the pellet stored at −20 °C. The cells were lysed in 50 mM Tris pH 7.4 containing 2 mg/mL lysozyme, 2 mM EDTA, 2 mM DTT, 1% Triton, and supplemented with EDTA-free protease inhibitor cocktail by ultrasonication (UP50H, Ultrasonic processor, Hielscher ultrasound technology) for 5 cycles of 1 min pulsing and 2 min resting on ice, and finally with a Potter homogenizer until the suspension no longer appeared viscous. The homogenized suspension was centrifuged at 4 °C for 45 min at 14,800*g* and the supernatant removed and filtered through a 0.45 μm syringe filter (Millex® Syringe-driven filter unit, Millipore, Watford, UK). The GST-tagged PTEN was purified with a gravity flow column packed with 5 mL of glutathione sepharose 4B beads (GE Healthcare, Little Chalfont, UK) previously equilibrated with 50 mM Tris pH 7.4, 140 mM NaCl, 2.7 mM KCl (Tris column buffer). All purification steps were performed at 4 °C. The filtered cell extract was loaded onto the column and allowed to flow through by gravity. A series of reducing saline wash buffers were then loaded onto the column in the following order: 25 mL of Tris column buffer containing 1% Triton X-100 and 2 mM DTT; 40 mL of Tris column buffer containing 2 mM DTT; 40 mL of 50 mM Tris pH 7.4, 500 mM NaCl, 2.7 mM KCl, 2 mM DTT. The protein was eluted by overnight incubation of the column in 50 mM Tris pH 7.4, 20 mM reduced L-glutathione, 250 mM NaCl, 2 mM DTT, and an equal volume of glycerol was added to the eluent for storage at −80 °C. Prior to use the protein was buffer-exchanged in 20 mM

Tris pH 7.4, 0.1 mM EDTA, 100 mM NaCl using a Microcon® 10 kDa Centrifugal filter unit (Millipore, Watford, UK), according to the manufacturer's recommendations. Protein concentration was determined using absorbance at 280 nm with a Nanodrop 2000c UV–vis Spectrophotometer (Thermo Scientific, Hemel Hemstead, UK).

2.3. PTEN oxidation and activity assay

Purified buffer-exchanged PTEN-GST was treated with either 0 or 1 mM H_2O_2 for 1 h at room temperature. The reaction was quenched by the addition of 5 mM methionine. An aliquot of the 1 mM H_2O_2 oxidized sample was subsequently incubated in 100 mM DTT for 15 min to assess the reversibility of the oxidation. The phosphatase activity of PTEN was measured by monitoring the hydrolysis of the artificial substrate 3-*O*-methylfluorescein phosphate (OMFP) to 3-*O*-methylfluorescein (OMF). Fresh OMFP was prepared in dimethyl sulfoxide (DMSO) to a final concentration of 20 mM. 60 μg each of untreated, oxidized and DTT-treated oxidized protein were mixed with 10x Assay Buffer (150 mM Tris pH 7.4, 10 mM EDTA, 750 mM NaCl) according to Tierno et al. [27]. The 20 mM OMFP substrate mixture was diluted 25-fold with 1 M Tris pH 7.4 and added to the final assay mixture containing the protein. The released OMF fluorescence was determined with excitation at 485 nm, emission at 525 nm and cutoff at 515 nm continuously over 20 min using a Spectra MAX GEMINI XS Fluorescence plate reader (Molecular Devices Sunnyvale, CA, USA) controlled with the Softmax Pro® software. A standard curve generated by reading serial dilutions of OMF was used to determine protein specific activity. Statistical analysis of activity data was performed using GraphPad Prism Software (GraphPad, San Diego, CA, USA) using one-way ANOVA followed by Tukey's multiple comparison test.

2.4. Cell culture

HCT116 human colon cancer cells were grown in Dulbecco's modified Eagle medium (41966, Life Technologies, Paisley, UK) supplemented with 10% fetal bovine serum (Life Technologies, Paisley, UK) and maintained at 37 °C, 5% CO_2 in a controlled incubator. Approximately $5x10^7$ cells of passage 4–10 were harvested, washed twice with ice cold phosphate buffered saline (PBS) pH 7.4 by spinning at 500*g* for 10 min, and lysed with ice cold 50 mM Tris pH 7.4 containing 150 mM NaCl, 1 mM EDTA, 0.5% NP-40 (Sigma Aldrich Chemical Co., Dorset, UK) supplemented with EDTA-free protease inhibitor cocktail (Catalog no. 11 873 580 001, Roche Diagnostics GmbH, Mannheim, Germany) by incubating for 45 min on ice with occasional mixing. The lysate was clarified by spinning at 20,000*g* for 15 min at 4 °C.

2.5. Preparation of PTEN affinity capture column and protein capture

The untreated and oxidized/DTT-recovered samples of PTEN-GST (100 μg protein each) were diluted in 500 μL of wash buffer (20 mM Tris pH 7.4, 0.1 mM EDTA, 100 mM NaCl) supplemented with 100 mM DTT; the oxidized PTEN-GST (100 μg) and a GST control (100 μg) were diluted in 500 μL of wash buffer without DTT. 100 μL of glutathione sepharose 4B slurry (GE Healthcare, Little Chalfont, UK) was sedimented by centrifugation at 500*g* for 5 min. The glutathione sepharose beads were extensively washed with wash buffer and stored at 4 °C. The bait proteins (GST or PTEN-GST) were immobilized on the glutathione sepharose beads by incubation with the protein solutions at 4 °C for 3 h. The beads were then washed once with wash buffer, and then 1 mL of HCT116 cell lysate derived from approximately 5×10^7 cells was incubated with each of the immobilized bait proteins and a control consisting of glutathione sepharose beads only, at 4 °C overnight on an end-over-end mixer. Subsequently, the beads were washed with 500 μL of 20 mM Tris pH 7.4, 0.1 mM EDTA, 300 mM NaCl, 0.5% NP-40 to remove non-bound proteins. For reducing gels the bound proteins were then eluted by boiling in SDS-PAGE Sample Buffer Laemmli 2 × concentrate, or for non-reducing gels in 2 × non-reducing SDS sample buffer (125 mM Tris pH 6.8, 4% SDS, 15% glycerol, 0.01% bromophenol blue), and analyzed by SDS-polyacrylamide gel electrophoresis followed by staining with Coomassie Brilliant Blue.

2.6. Protein digestion

Gels run under reducing conditions were stained with InstantBlue (Expedeon, Cambridge, UK), to visualize the lanes prior to further processing. The gel lanes corresponding to the bead control, the GST control, the untreated (reduced) PTEN-GST and the oxidized PTEN-GST samples were then each cut into 12 slices. The gel pieces were washed twice with 500 μL 100 mM NH_4HCO_3 and twice with 100 mM NH_4HCO_3/50% acetonitrile. Reduction was performed adding 10 μL of 45 mM DTT to 150 μL NH_4HCO_3 and incubating at 60 °C for 30 min. Cysteine alkylation was performed by adding 10 μL of 100 mM iodoacetamide and incubating at room temperature for 30 min in the dark. The gel pieces were washed in 100 mM NH_4HCO_3/50% acetonitrile and incubated in 50 μL of 100% acetonitrile for 10 min. The gel pieces were then dried completely in a centrifugal evaporator and resuspended in 25 μL of 0.1 μg/μL trypsin (Trypsin Gold, Mass Spectrometry Grade, Promega, Southampton, UK) in 50 mM acetic acid. 100 μL 40 mM NH_4HCO_3/10% acetonitrile was added to the gel pieces, which were incubated overnight at 37 °C. The gel pieces were pelleted by centrifugation and the supernatant was collected in a fresh tube. Peptide extraction from the gel pieces was performed by adding 20 μL 5% formic acid and incubating at 37 °C for 20 min, followed by addition of 40 μL acetonitrile and incubation for 20 min at 37 °C. The gel pieces were pelleted by centrifugation, and the supernatant was combined with the first extract; this procedure was repeated twice. The peptide extracts were dried completely in a vacuum centrifuge and resuspended in a volume up to 50 μL of 98% H_2O, 2% acetonitrile, 0.1% formic acid (HPLC solvent A) and loaded into screw top glass autosampler vials (Chromacol, Speck and Burke analytical, Clackmannanshire, UK).

2.7. LC–MS

Peptides were separated and analyzed using an Ultimate 3000 system (Thermo Scientific, Hemel Hemstead, UK) coupled to a 5600 TripleTOF (ABSciex, Warrington, UK) controlled by Chromeleon Xpress and Analyst software (TF1.5.1, ABSciex, Warrington, UK). Enrichment and desalting of the peptides was achieved using a C18 pre-column (C18 PepMap™, 5 μm, 5 mm × 0.3 mm i.d., Thermo Scientific, Hemel Hemstead, UK) washing for 4 min with aq. 2% acetonitrile, 0.1% formic acid at 30 μL/min. The peptides were then separated on a C18 nano-HPLC column (C18 PepMap™, 5 μm, 75 μm i.d. × 150 mm, Thermo Scientific, Hemel Hemstead, UK) at 300 nL/min using a gradient elution running from 2% to 45% aqueous acetonitrile (0.1% formic acid) over 45 min followed by a washing gradient from 45% to 90% aq. acetonitrile (0.1% formic acid) in 1 min. The system was washed with 90% aq. acetonitrile (0.1% formic acid) for 5 min and then re-equilibrated to the starting solvent. Ionization of the peptides was achieved with spray voltage set at 2.4 kV, a source temperature of 150 °C, declustering potential of 50 V and a curtain gas setting of 15. Survey scans were collected in positive mode from 350 to 1250 Da for 200 ms using the high resolution TOF-MS mode. Information-dependent acquisition (IDA) was used to collect MS/MS data using the following criteria: the 10 most intense ions with +2 to +5 charge states and a minimum of intensity of 200 cps were chosen for analysis, using

dynamic exclusion for 12 s, and a rolling collision energy setting.

To calculate the relative abundance of a given modified residue, the individual abundance values of each detected peptides containing the amino acid in both its modified and unmodified form were added together. Next, the abundances of the detected peptides containing the residue solely in its modified form were summed and divided by the total abundance value to obtain the relative abundance of the modification. Statistical analysis of activity data was performed with GraphPad Prism Software (GraphPad, San Diego, CA, USA) using two-tailed unpaired Student's *t* test (for multiple comparisons). $p < 0.05$ was considered significant.

2.8. Label-free quantification with Progenesis QI for proteomics

Comparative quantification was performed using the Progenesis QI for Proteomics software (Non-linear Dynamics, Newcastle, UK). A total of 12 experiments were created, one for each set of gel bands excised from the lanes of the Coomassie-stained gel at the same molecular weight. For each experiment, LC–MS runs corresponding to peptides digested from each band across the lanes and corresponding to the proteins bound to the reduced and oxidized PTEN-GST were aligned against each other. The alignment reference was automatically chosen by the software and after automated alignment of the data additional vectors were added manually where necessary to improve the initial alignments. The feature normalization was set to normalize to all proteins, the automatic sensitivity method of the peak picking algorithm was set at default and the maximum allowable ion charge was set at 20. No peptide ion filtering was applied. The experimental design setup was set as Between-subject Design. The spectra were exported in .mgf format for database searching, and the search results were imported in .xml format after Mascot Database search for the identification of matched peptides. Any peptide showing a Mascot ion score below the threshold indicative of identity or extensive homology (p value < 0.05) was removed from the feature identification list. Cytoskeletal keratin IDs were removed from the feature identification list. Only features that showed zero conflicts were used for quantification. Data obtained from the alignment of LC–MS runs correspondent to single fractions were then pooled into a multi-fraction experiment. Statistical analysis was performed using Progenesis QI for Proteomics using a one-factor ANOVA.

2.9. Database search

The Mascot® probability based search engine (Matrix Science, London, version 2.4.0) was used to interrogate SwissProt 2015-03 primary database [28]. For Mascot searches that was not automated through the Progenesis QI analysis, LC–MS .wiff file were converted into .mgf format using Peakview® (AB SCIEX). The 12 . mgf files obtained the Progenesis analysis of each of the samples were searched for protein identification and for bait protein oxidative post-translational modifications (oxPTMs). For protein identification, a variable modification of methionine oxidation and a fixed modification carbamidomethyl cysteine were used. For the analysis of the oxPTMs of the bait, the variable modification lists included: methionine oxidation and dioxidation; cysteine oxidation, dioxidation and trioxidation, and tyrosine oxidation. Other parameters for the searches were as follows: Enzyme: Trypsin; Peptide tolerance: ± 0.8 Da; MS/MS tolerance: ± 0.8 Da; Peptide charge state: $+2$, $+3$ and $+4$; Max Missed cleavages: 1; #13C: 1; Quantitation: None; Instrument: ESI-QUAD-TOF; Data format: Mascot Generic; Experimental mass values: Monoisotopic; Taxonomy *Homo sapiens* (Human).

2.10. Validation by Western blotting

Proteins resolved by SDS-PAGE were transferred onto PVDF membrane (Immobilion-P, Millipore, Watford, UK) in 25 mM Tris pH 8.3, 192 mM glycine, 10% methanol applying 30 V overnight at 4 °C. The membrane was blocked in Tris buffered saline (TBS)-Tween blocking buffer (20 mM Tris pH 7.6, 137 mM NaCl, 0.05% Tween-20, 5% BSA) for 1 h, incubated in blocking buffer with monoclonal primary antibodies for Trx, Prdx1, Anxa2, or DDB1 at the working dilution of 1:1000 overnight at 4 °C, washed extensively for 30 min (3 washes of 10 min each) with TBS-Tween and incubated with either HRP-linked anti-mouse or HRP-linked anti-rabbit secondary antibodies (working dilution 1:1000) for 1 h at room temperature. The membrane was washed again as described above and HRP-linked anti-mouse or HRP-linked anti-rabbit were detected using Life Technologies ECL kit according to the manufacturer's instructions. The membrane was scanned using a G:BOX system (Syngene, Cambridge, UK) running the GeneSys software (Syngene, Cambridge, UK). Next, the membrane was stripped in Restore Plus Stripping buffer (Life Technologies, Paisley, UK) for 15 min, washed as described above and reblocked in TBS-Tween plus 5% BSA. The monoclonal primary antibodies for PTEN was incubated with the stripped membrane in blocking buffer at the working dilution of 1:2500 for 1 h at room temperature, the membrane washed, and incubated with HRP-linked secondary antibody for 1 h at room temperature at the working dilution of 1:2500. After washing, HRP-linked antibody detection and scanning procedures were repeated as described above.

3. Results

3.1. Confirmation of reversible disulfide bond formation of H_2O_2-oxidized PTEN-GST

Purified PTEN-GST was prepared in the presence of high levels of DTT to maximize retention of catalytic activity, but was exchanged into non-reducing buffer prior to treatment with H_2O_2 to allow oxidation. The buffer exchange had no significant effect on the catalytic activity, as monitored by the OMFP phosphatase assay (Supplementary Fig. 1). The effect of oxidation *in vitro* with 1 mM H_2O_2 on PTEN activity was measured using the OMFP phosphatase assay immediately before the immobilization of the bait protein onto glutathione sepharose beads. When PTEN was treated with 1 mM H_2O_2 for 1 h, the phosphatase activity dropped dramatically, but was recoverable by subsequent incubation with 100 mM DTT (Fig. 1). This confirmed that the oxidative inactivation was reversible, and is consistent with it being due to formation of an intramolecular disulfide bond between the catalytic cysteine Cys124 and regulatory cysteine Cys71 in the active site of the enzyme, as reported previously [10]. This reduced protein was used as a control in subsequent IP experiments as it should retain any non-reversible oxidation.

3.2. Identification of proteins affinity-captured by the reduced and oxidized PTEN-GST

The untreated PTEN bait protein was maintained in reducing conditions (100 mM DTT) during the immobilization step to prevent spontaneous oxidation, and to ensure direct correlation between PTEN redox status (reduced *versus* oxidized) and the results of the protein interaction analysis. However, no reducing agent was added to the HCT116 cell lysate used for the affinity-capture, in order to avoid further alteration of the redox status of potential interactors. Care was taken to keep the amount of protein immobilized consistent across the different baits used. The

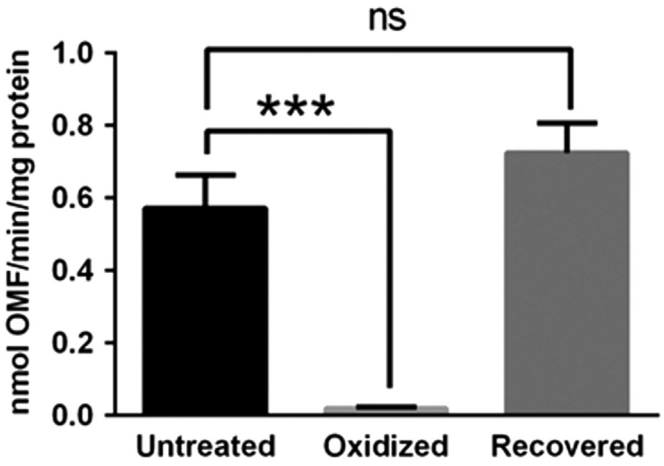


Fig. 1. Effect of 1 mM H_2O_2 oxidation on PTEN-GST phosphatase activity. The untreated, oxidized and DTT-incubated PTEN-GST were assayed for phosphatase activity using the *O*-methylfluorescein phosphate assay, immediately before the immobilization step. The results are presented as mean ± SD ($n=3$) of PTEN specific activity. Statistical significance was assessed by one-way ANOVA followed by Tukey's multiple comparison test. The enzymatic activity of PTEN-GST following 1 mM H_2O_2 oxidation is significantly different to that of the untreated PTEN-GST ($p=0.0002$). The enzymatic activity of the untreated protein is not significantly different to that obtained following incubation of the oxidized PTEN-GST with 100 mM DTT ($p=0.0861$). The calculated specific activity values are 0.5720 ± 0.0917 nmol OMF/min/mg protein for the untreated PTEN-GST; 0.0206 ± 0.0031 nmol OMF/min/mg protein for the H_2O_2-oxidized PTEN-GST and 0.7249 ± 0.0819 nmol OMF/min/mg protein for the PTEN-GST following 15 min incubation with 100 mM DTT. $^{***}p<0.001$; ns=not significant.

glutathione sepharose beads alone and with immobilized GST were also incubated with HCT116 lysate as negative controls. Proteins captured by the immobilized native and oxidized PTEN-GST bait and the controls mentioned above were initially analyzed by SDS-PAGE (Supplementary Fig. 2). Although there were limited bands visible in the Coomassie stained gel, small differences were observed in the oxidized PTEN-GST sample lane compared to the native PTEN-GST and GST and beads controls, especially for proteins between 50 and 60 kDa. The wash following bait immobilization was also analyzed in order to test the binding efficiency of the reduced and the oxidized PTEN-GST to the glutathione sepharose beads. The results (Supplementary Fig. 2) suggest that in all cases we were able to saturate the resin for the affinity-capture, as traces of PTEN-GST were visible in the gel lanes loaded with the wash buffer from resin loaded with both reduced and oxidized PTEN-GST, reflecting the elution of unbound PTEN-GST.

Each gel lane was dissected into 12 approximately equal slices, trypsin digested and analyzed by LC–MS. Mascot (Matrix Science, v. 2.4.0) was used to identify proteins from all samples, and Progenesis QI for Proteomics software was used for label-free quantification analysis of the LC–MS data for the proteins bound to the reduced and the oxidized PTEN-GST samples. A total of 237 proteins were identified after Mascot database search of the data. The bait protein PTEN and its GST protein tag were identified with a high level of confidence in both reduced and oxidized fractions. Proteins that were also found in the bead and GST controls were removed from the list but are included in Supplementary Table 1. Of the 97 identified proteins from the remaining list, 27 that showed a confidence score above 50 and a number of unique peptides greater than or equal to 2 and *p*- and *q*-values < 0.05 for the quantification are reported in Table 1. The 70 proteins that showed a confidence score above 50 and a number of unique peptides greater than or equal to 2 but a *q*-value > 0.05 are shown in Supplementary Table 2, and those that were below this cutoff criteria are listed in Supplementary Table 3. The overall false discovery rate reported by Mascot was 2.1%, which is reasonable for a small dataset.

Some of the interactors identified are highly abundant cellular proteins and have been reported before to show non-specific binding to beads, although they were not present in the controls in this study. These proteins included elongation factors, tubulin, myosins, histones, 60S and 40S ribosomal proteins, and heat-shock proteins; interestingly, almost all of these have been reported as interactors in previous proteomics studies of the PTEN interactome [29,30].

3.3. Potential novel interactors of PTEN

Some of the proteins identified as interactors correspond to proteins not previously identified as PTEN-binding proteins; these are indicated by "e" in Table 1. Known interactors not commonly identified as associating with beads are indicated by "f" in the table. While no direct interaction of these proteins with PTEN has been shown to date, some of them are linked with the cellular pathways in which PTEN is known to be involved. A number are involved in DNA replication and DNA damage, including protein pelota analog (Pelo), DNA-damage binding protein 1 (DDB1) and polymerase delta-interacting protein 2 (PDIP2 or Poldip2). There are also a number of proteins associated with cytoskeletal structure and control, including spectrin α-chain (Spta1), myosin phosphatase Rho-interacting protein (MPRIP) and desmoplakin (Dsp). Other interesting potentially novel interactors include the multi-enzyme fatty acid synthase (FAS), A-kinase anchor protein 12 (AKAP12), and guanine nucleotide-binding protein G(i) subunit α and/or β (GNAIα/β).

3.4. PTEN binding proteins interact differently with reduced and oxidized PTEN-GST baits

Of the interactors identified, 14 showed a significant change in binding on oxidation-induced inactivation of the PTEN-GST bait, with *p*- and *q*-values < 0.05 and greater than 2.5 fold change (Table 1, bold entries). These interactors were all manually validated to confirm the quality of the identification and quantitative data; for example, annexin A2 (Anxa2, 6.8-fold change, *p*-value = 0.0118), PDIP2 (10.8-fold change, *p*-value < 0.0001) and the actin-binding protein drebrin (Drb1) (4.8-fold change, *p*-value = 0.0180) showed substantially increased binding to the H_2O_2 oxidized PTEN-GST.

Two proteins that showed high fold changes in binding to oxidized PTEN-GST were thioredoxin and thioredoxin peroxidase (peroxiredoxin-1; Prdx1), both of which are proteins with redox functions. A total of 6 Prdx1 peptides were detected, of which 5 unique peptides were used for quantification. Prdx1 was significantly more abundant in the sample eluted from the oxidized PTEN-GST than in the sample eluted from the reduced PTEN-GST (4.1-fold change, *p*-value = 0.0233). Two unique Trx peptides were detected, and the protein was significantly more abundant (6.2-fold change, *p*-value = 0.0065) in the protein fraction eluted from the oxidized PTEN-GST. Using Progenesis QI for proteomics we were able to verify the presence of the peptide features corresponding to the identified proteins listed in Table 1 and compare their intensities. Fig. 2 shows the three-dimensional maps zoomed into the features corresponding to the Prdx1 and the Trx peptides detected following elution of the proteins bound to the oxidized and reduced PTEN-GST baits.

3.5. Validation of selected interactions with Western blotting confirmed the proteomics study

Following screening of the identified proteins and alterations in

Table 1
Identification and LC–MS based label free quantification of the binding partners of reduced and 1 mM H_2O_2 oxidized PTEN following GSH affinity enrichment.

Accession[a]	Peptide count[b]	Confidence score[c]	*p*-Value[d]	*q*-Value[d]	Fold change[d]	Highest mean condition	Protein description
PDIP2_HUMAN	**4 (4)**	**190.31**	**< 0.0001**	**0.0005**	**10.8**	**Oxidized**	**Polymerase delta-interacting protein 2[e]**
PELO_HUMAN	**2 (2)**	**110.35**	**0.0018**	**0.0212**	**2.7**	**Oxidized**	**Protein pelota homolog[e]**
RS2_HUMAN	2 (2)	97.3	0.0021	0.0212	1.9	Oxidized	40S ribosomal protein S2[f]
RL10A_HUMAN	**2 (2)**	**71.19**	**0.0014**	**0.0212**	**5.3**	**Reduced**	**60S ribosomal protein L10a[f]**
RLA0_HUMAN	3 (3)	159.13	0.0052	0.0261	2.4	Oxidized	60S acidic ribosomal protein P0[f]
THIO_HUMAN	**2 (2)**	**150.69**	**0.0065**	**0.0299**	**6.2**	**Oxidized**	**Thioredoxin**
SSRD_HUMAN	2 (2)	153.39	0.0075	0.0301	1.7	Reduced	Translocon-associated protein subunit delta[e]
ANXA2_HUMAN	**3 (3)**	**195.41**	**0.0118**	**0.0374**	**6.8**	**Oxidized**	**AnnexinA2**
FAS_HUMAN	3 (3)	163.01	0.0144	0.0387	1.7	Oxidized	Fatty acid synthase[e]
AKA12_HUMAN	4 (4)	180.42	0.0181	0.0415	1.3	Oxidized	A-kinase anchor protein 12[e]
DREB_HUMAN	**2 (2)**	**83.3**	**0.018**	**0.0415**	**4.9**	**Oxidized**	**Drebrin**
PRDX1_HUMAN	**6 (5)**	**316.76**	**0.0233**	**0.0437**	**4.1**	**Oxidized**	**Peroxiredoxin-1**
DESP_HUMAN	4 (4)	165.62	0.0221	0.0437	1.6	Oxidized	Desmoplakin[e]
NDKA_HUMAN	3 (3)	131.93	0.026	0.0448	1.5	Oxidized	Nucleoside diphosphate kinase A[e]
DHB8_HUMAN	**2 (2)**	**110.35**	**0.0258**	**0.0448**	**6.4**	**Oxidized**	**Estradiol 17-beta-dehydrogenase 8[e]**
UTRO_HUMAN	2 (2)	101.72	0.0306	0.0454	2.2	Oxidized	Utrophin[e]
SPTN1_HUMAN	**4 (4)**	**188.58**	**0.0361**	**0.0456**	**2.9**	**Oxidized**	**Spectrin alpha chain, non-erythrocytic 1[e]**
RS9_HUMAN	4 (4)	172.02	0.0331	0.0456	1.5	Oxidized	40S ribosomal protein S9[f]
RL38_HUMAN	5 (5)	405.89	0.0389	0.0463	1.6	Oxidized	60S ribosomal protein L38[f]
GNAI1_HUMAN	**6 (4)**	**343.46**	**0.0462**	**0.0463**	**3.6**	**Oxidized**	**Guanine nucleotide-binding protein G(i) subunit alpha-1[e]**
GNAI2_HUMAN	**5 (2)**	**300.5**	**0.0488**	**0.0463**	**6.9**	**Oxidized**	**Guanine nucleotide-binding protein G(i) subunit alpha-2[e]**
MPRIP_HUMAN	4 (4)	164.53	0.0423	0.0463	2.1	Oxidized	Myosin phosphatase Rho-interacting protein[e]
RS15A_HUMAN	**3 (2)**	**135.35**	**0.0449**	**0.0463**	**0.7**	**Oxidized**	**40S ribosomal protein S15a[f]**
GSTM2_HUMAN	2 (2)	130.8	0.0495	0.0463	1.4	Reduced	Glutathione S-transferase Mu 2[e]
SKP1_HUMAN	**2 (2)**	**112.83**	**0.0413**	**0.0463**	**8.6**	**Oxidized**	**S-phase kinase-associated protein 1**
HSP7C_HUMAN	**2 (2)**	**107.77**	**0.0413**	**0.0463**	**3.0**	**Oxidized**	**Heat shock cognate 71 kDa protein**
EF2_HUMAN	2 (2)	101.61	0.0428	0.0463	1.3	Oxidized	Elongation factor 2[f]

The data was obtained from the analysis of three independent GSH-affinity experiments. The list was restricted to the protein hits showing a confidence score ≥ 50 and a number of unique peptides ≥ 2 and a *p*- and *q*-value < 0.05. Ranking is based on *q*-values.
Bold indicates more than 2.5-fold change in abundance depending on PTEN redox status.

[a] Accession = SwissProt Protein ID.
[b] Peptide count = the number of detected peptides (the number of unique peptides) used for quantification.
[c] The protein confidence score was generated using Mascot as described in the experimental methods.
[d] The *p*-value, *q*-value and fold change were generated by Progenesis QI for proteomics as described in the experimental methods.
[e] Indicates proteins not previously identified as PTEN interactors.
[f] Indicates proteins that appeared to be PTEN interactors (*i.e.* were not found in controls) but have also been found as common non-specific interactors in bead-based affinity enrichments.

their abundance between the sample eluted from the reduced and oxidized bait, a number of the more interesting interactors were selected for validation by Western blot, in order to confirm the interaction and the quantitative changes in binding to oxidized PTEN-GST. The GSH-affinity capture was performed with the DTT-recovered oxidized PTEN-GST as additional control for the validation of interactors. Prdx1, Trx, and Anxa2 were chosen for validation from the interactors that had altered binding to PTEN, and DDB1 as a novel interactor from those with unaltered binding, and their levels were compared across the protein samples eluted from the reduced, oxidized and DTT-recovered PTEN-GST against PTEN loading control (Fig. 3). For all the proteins selected, the Western blot results were in agreement with the proteomics data and confirmed the comparative quantitative analysis between the oxidized and reduced sample. The levels of Prdx1 (Fig. 3A), Trx (Fig. 3B) and Anxa2 (Fig. 3C) were visibly increased in the sample eluted from the H_2O_2-oxidized PTEN. Little or no signal was observed for those proteins in the samples corresponding to the reduced (untreated) and DTT-recovered PTEN, confirming, at a qualitative level, the significant difference observed by MS-based label-free quantification. No significant change in the levels of DDB1 were observed (Fig. 3D), again in agreement with the proteomics-based analysis. None of the chosen interactions was detected in the samples eluted from the immobilized GST control nor from the glutathione sepharose beads alone.

3.6. Non-reducing gels to test for intermolecular disulfide formation

To explore the possibility that the association between proteins was mediated by intermolecular disulfide formation, the Western blot validation was also performed on non-reducing gels (Supplementary Fig. 4). If disulfide formation was responsible for the association then a band that blotted for both PTEN-GST and the associated protein should appear at the additive mass of the two proteins; specifically, 112 kDa for Anxa-2-PTEN-GST, 96 kDa for Prdx1-PTEN-GST, and 86 kDa for Trx-PTEN-GST. No bands were identified at these masses (as indicated in Supplementary Fig. 4). Some additional bands were apparent, but these appear to be oligomers of the captured proteins.

3.7. Relative quantification of oxPTMs of the oxidized PTEN-GST bait

After quantification and validation of the affinity-captured interactors, a Mascot database search was performed on the aligned LC–MS runs to check for any oxidative post-translational modifications (oxPTMs) that occurred to the PTEN-GST bait following oxidation with hydrogen peroxide and affinity capture of protein–protein interactions, and might also have affected any interactions. Given the concentration of hydrogen peroxide used to inactivate PTEN (1 mM), we did not expect the treatment to generate major modifications other than the formation of the Cys71–Cys124 disulfide bond. The aligned features identified across three

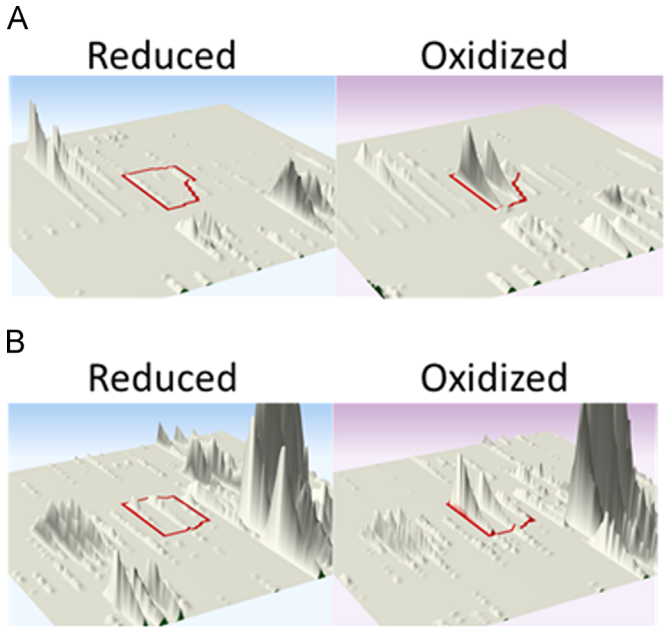


Fig. 2. Representative 3D montage of the comparative MS-based label free quantification for the peroxiredoxin-1 peptide TIAQDYGVLK and the thioredoxin-1 peptide TAFQEALDAAGDK detected following elution of the proteins bound to the reduced and oxidized PTEN-GST. The montages are representative of three independent experiments. (A) The Prdx1 peptide TIAQDYGVLK (m/z=554.30, 2+; RT=22.24 min) was found to be 4.2 times more abundant in the sample obtained from the oxidized PTEN GST than in the sample obtained from the reduced PTEN-GST (one-factor ANOVA, p-value=0.0358, n=3). (B) The Trx peptide TAFQEALDAAGDK (m/z=668.83, 2+; RT=24.45 min) was found to be 7.33 times more abundant in the sample obtained from the oxidized PTEN GST than in the sample obtained from the reduced PTEN-GST (one-factor ANOVA, p-value=0.0107, n=3).

independent GSH-affinity enrichment experiments were searched for methionine oxidation and dioxidation, cysteine oxidation, dioxidation and trioxidation, and tyrosine oxidation. A total of 4 PTEN peptides and 6 GST peptides were found to be oxidatively modified (Table 2). Interestingly, Met134 of PTEN was substantially oxidized in both control and oxidized PTEN, but there was no significant difference between the two, and a number of GST peptides also showed significant oxidation in both samples. The only significant increase in oxidation following treatment was at Met35 of PTEN in the peptide YQEDGFDLDLTYIYPNIIAMGFPAE. Overall, these results suggest that apart from the formation of the regulatory disulfide, the oxidative treatment caused minimal additional oxidative modifications to the PTEN-GST.

4. Discussion

In this study we have carried out the first comprehensive analysis of the redox proteome of PTEN. We have identified a number of proteins whose interaction with PTEN appears to be dependent on the PTEN redox status, specifically, increased for oxidized PTEN, and we have also identified a number of potentially novel PTEN interactors.

The observed >95% oxidative-induced inactivation of the bait protein was in agreement with previous studies reporting the effect of 1 mM H_2O_2 on PTEN phosphatase activity [12], and the DTT-induced reversibility of the inhibitory effect is good evidence of the involvement of the regulatory disulfide in PTEN-GST inactivation, as previously discussed by Lee et al. [10]. The oxidant type and concentration were chosen to maximize the formation of the regulatory disulfide bond between Cys71 and Cys124 while minimizing oxidation of other amino acids. It is important to bear in mind that the concentration of H_2O_2 used to generate the PTEN disulfide in the *in vitro* studies described here may differ significantly from that needed to show similar effects *in vivo*, and the use of exogenous H_2O_2 in studying signal transduction needs to be undertaken with some care [31]. Mass spectrometric analysis and quantification of oxidation of susceptible amino acids (methionine, cysteine) indicated that treatment with 1 mM H_2O_2 caused very little change in the oxidation levels of oxidation of PTEN or GST, apart from a small increase in the oxidation of one residue, Met35

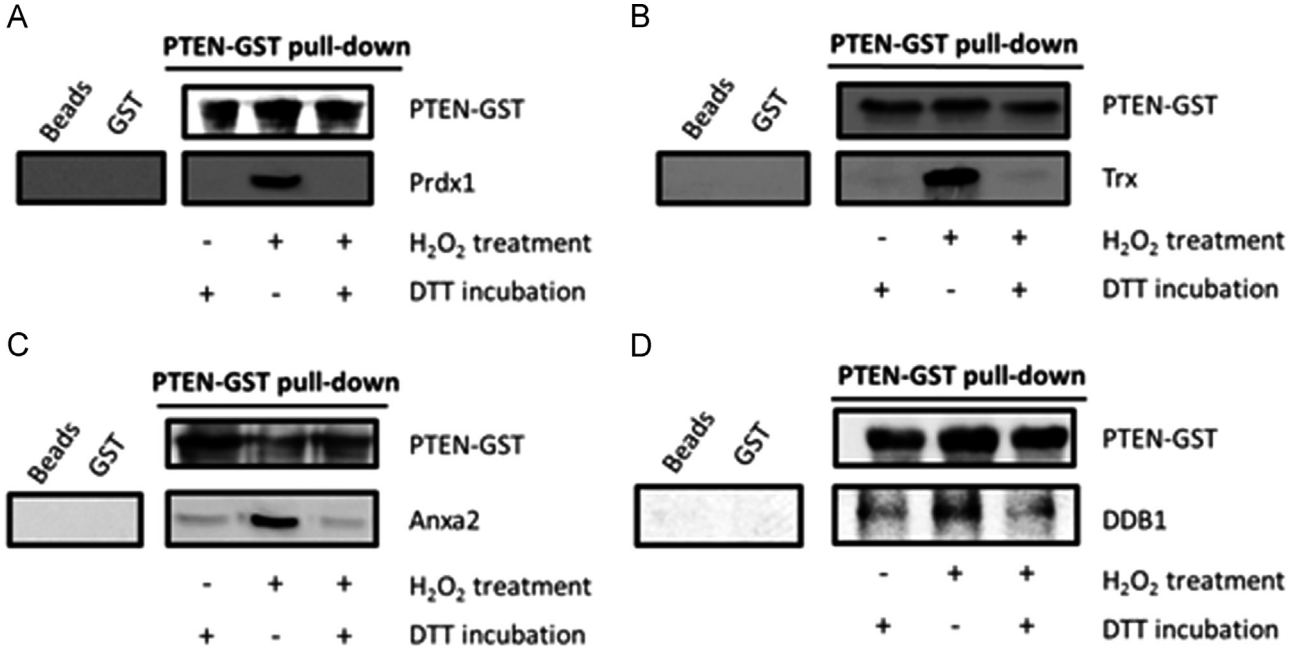


Fig. 3. Western blots showing validation of proteomics data in comparing selected affinity-captured PTEN interactions across the samples eluted from untreated, oxidized and DTT-recovered PTEN-GST. Each panel shows PTEN-GST loading control; expression of selected PTEN-interactor in the H_2O_2-treated, untreated and recovered PTEN-GST pull down compared to the sample eluted from GST and beads alone; whether the bait was treated with 1 mM H_2O_2 and/or incubated with 100 mM DTT. Both untreated and recovered samples were kept in constant reducing conditions (100 mM DTT incubation) during the bait immobilization and showed similar interactions profile. The H_2O_2-treated PTEN-GST pull down showed increased level of Prdx1 (A), Trx (B) and Anxa2 (C) and comparable levels DDB1 (D) when compared to the reduced controls.

Table 2
Identification and quantification of PTEN and GST oxidative modifications in comparing untreated *versus* 1 mM oxidized PTEN-GST following GSH-affinity enrichment.

Protein	Peptide sequence[a]	Fraction detected[b]	*m/z* (charge)	Modifications[c]	*p*-Value[d]	% Relative modification	
						Reduced	Oxidized
PTEN	YQEDGFDLDLTYIYPNIIA*M*GFPAER	5	1023.2028 (3)	Met 35 OX	**0.0004**	1.01 ± 1.74	14.48 ± 1.28
PTEN	TGVM*I*CAYLLHR	3	470.2714 (3)	Cys 136 DIOX	0.420748	2.31 ± 0.60	1.63 ± 1.17
PTEN	TGVM*I*CAYLLHR	2,3,4	483.9500 (3)	Met 134 OX	0.696349	34.05 ± 3.61	30.64 ± 13.64
PTEN	F*M*YFEFPQPLPVCGDIK	3	1052.5630 (2)	Met 239 OX	0.959338	1.76 ± 3.05	1.65 ± 1.61
GST	*M*LLADQGQSWK	6,7,8,9,10,11	646.8266 (2)	Met 20 OX	**0.0333**	24.59 ± 3.69	17.79 ± 0.19
GST	*M*LLADQGQSWK	7,10	431.5445 (3)	Met 20 OX	**0.0487**	24.33 ± 2.01	21.00 ± 0.46
GST	*M*LLADQGQSWK	7	654.8150 (2)	Met 20 DIOX	0.0681	0.39 ± 0.12	0.21 ± 0.03
GST	ASCLYGQLPK	7	556.2746 (2)	Cys 48 DIOX	0.0705	1.80 ± 0.69	0.65 ± 0.44
GST	ASCLYGQLPK	7	564.2732 (2)	Cys 48 TRIOX	0.2220	0.89 ± 0.42	1.59 ± 0.73
GST	PP*Y*TVVYFPVR	7	677.3622 (2)	Tyr 4 OX	0.2590	0.76 ± 0.26	0.55 ± 0.05
GST	DQQEAALVD*M*VNDGVEDLR	7,8,9,10	1067.0113 (2)	Met 92 OX	0.3008	30.14 ± 11.34	22.27 ± 1.78
GST	*M*LLADQGQSWKEEVVTVETWQEGSLK	10	752.6226 (4)	Met 20 OX	0.5333	13.07 ± 3.68	14.88 ± 2.78
GST	*M*LLADQGQSWKEEVVTVETWQEGSLK	9,10	1003.1702 (3)	Met 20 OX	0.5981	18.41 ± 1.64	19.83 ± 3.96
GST	DQQEAALVD*M*VNDGVEDLR	7,8,9,10	711.6659 (3)	Met 92 OX	0.6981	26.70 ± 6.68	25.03 ± 1.97
GST	*M*PPYTVVYFPVR	7	495.5891 (3)	Met 1 OX	0.7441	19.89 ± 4.56	18.93 ± 1.39
GST	DQQEAALVD*M*VNDGVEDLR	7	533.9936 (4)	Met 92 OX	0.9933	44.85 ± 21.58	44.97 ± 9.42

The data was obtained from the analysis of PTEN and GST peptide features present in three independent GSH-affinity experiments. Ranking is based on *p*-values returned by Two-tailed unpaired Student's *t* test.

[a] Peptide sequence obtained from the Mascot database search of LC–MS runs aligned on Progenesis QI for Proteomics.
[b] Gel slice fraction(s) corresponding to the LC–MS run where the peptide was detected.
[c] Modification type and position within the protein amino acid sequence.
[d] *p*-Value returned by Two-tailed unpaired Student's *t* test, following relative quantification of the modifications.

of PTEN, to around 14% (Table 2); this residue is distant from the active site and not surface accessible. Given this, and the full restoration of the activity of the oxidized protein on DTT treatment, it is reasonable to assume that this modification was not responsible for the loss of function. It also seems unlikely that it contributed significantly to the observed changes in PTEN interacting proteins, especially as the changes in interactions were reversible by DTT according to the Western blotting validations.

HCT116 cells were chosen as a source of prey proteins for the affinity capture as this cell line has previously been demonstrated to be a suitable model to study the action of PTEN, as it is a widely-used epithelial cell cancer model, has two wild-type alleles of PTEN, and haploid and diploid knockouts are available for downstream mechanistic studies [32,33]. Cells were grown under normal conditions to assess the interactions affected by PTEN oxidation alone, and it is likely that lysates from stressed cells or other cell lines would show some differences in the interactome. Protein interactions were determined by MS-based proteomic techniques using immobilized PTEN in reduced and oxidized states along with appropriate controls. Four of the interactions, 3 redox sensitive (Prdx1, Trx, Anxa2) and 1 redox insensitive (DDB1), were confirmed by Western blotting. To rule out intermolecular disulfide formation through disulfide exchange with the PTEN being responsible for the interactions, the blotting was also performed from a non-reducing gel. If disulfide formation was responsible, a band that blots for both PTEN-GST and the target protein should be apparent at the combined mass of the proteins. These would be approximately 96 kDa for Prdx1, 86kDa for Trx and 122 kDa for Anxa2. There was no evidence of bands at these masses in the blots. In addition, intermolecular disulfide formation would be a relatively non-selective process and under equilibrium, hence one might expect rather more proteins to become disulfide bound to PTEN, especially the very abundant proteins with known reactive thiols such as GAPDH, SOD and the HSPs, and other abundant proteins that have been shown to form disulfides under oxidative stress conditions, such as actin and tubulin to be present in increased amounts in the oxidized sample (see for example [34]). The majority of the 93 interactors reliably identified show no change in binding between the samples, and the proteins with reactive thiols mentioned above either showed differences or were not present at all. Also, under the equilibrium conditions of the experiment, one might expect those proteins that have resolving thiols, such as PTEN and thioredoxin, where the equilibrium would lie to the intra rather than intermolecular disulfide (strong entropic drive), not to favor intermolecular disulfide formation. However, if intermolecular disulfides were formed between proteins under conditions of oxidative stress, this would be a good indication both of proximity and of redox sensitivity of the proteins, and the formation of these covalent associations could have significant implications for redox signaling.

It was interesting that significant increases in the binding of the redox proteins Prdx1 and Trx1 to the oxidized (inactive) PTEN-GST were observed. Prdx1 is a non-selenocysteine peroxidase that is known to catalyze the reduction of H_2O_2, protecting the cells from oxidative damage to DNA, lipids and proteins [35]. PTEN has previously been reported to interact with Prdx1, which seems to play a key role in protecting the phosphatase from H_2O_2-induced oxidative damage, as it fully restored PTEN activity in the presence of hydrogen peroxide [20]. Cao et al. suggested that Prdx1 binds PTEN through interaction with its C2 domain (aa 186–274), and they described a decreased binding of Prdx1 to PTEN when cells were treated with high concentration of H_2O_2 [20], which at first sight appears to conflict with the findings in our study. However, it has been proposed that this may be due to oxidative damage to Cys51 in Prdx1 resulting in dissociation of the PTEN/Prdx1 complex [20,36], and as our *in vitro* inactivation of PTEN does not involve direct oxidation of Prdx1, but rather the targeted formation of the regulatory disulfide, our data suggest that the binding of Prdx1 to PTEN is increased on formation of the regulatory disulfide. It is also possible that other interactors may contribute to the protection observed in cells and that it may be dependent on the presence of redox cofactors.

A second significant increase was seen for the antioxidant thioredoxin-1 (Trx). Trx, which also bound preferentially to oxidized PTEN bait protein, is generally thought to responsible for the reactivation of PTEN *via* reduction of the disulfide bond between Cys71 and Cys124 of PTEN with a thiol-disulfide exchange mechanism [10,11,37]. The increased abundance of Trx affinity captured with the oxidized PTEN-GST bait suggests that the formation of the PTEN:Trx complex is dependent on the redox status of PTEN.

It has been reported previously that redox status of Trx is also important in the PTEN/Trx interaction [19], as it was shown that reduced but not oxidized Trx binds the C2 domain of PTEN *via* a disulfide bond with PTEN Cys212, causing inhibition of the phosphatase and resulting in increased tumorigenesis. Overall, these findings imply that the redox status of both Trx and PTEN are important in the regulation of the interaction, and additional studies would be required to fully understand the dynamics of Trx-mediated PTEN reactivation *in vivo*.

Interestingly it has been shown that in macrophages treated with ATP, which results in the production of reactive oxygen species, PTEN is glutathionylated causing the activation of Akt and Erk1 [38], and both Trx and Prdx1 are also glutathionylated under oxidative stress conditions [39,40]. The enzymes responsible for the inactivation and reactivation of PTEN *via* glutathionylation have not been identified, but given the changing interactions of Trx and Prdx1 demonstrated in our study, it is possible that these enzymes are involved in this complex redox control.

PTEN has been shown to play an important role in the control of the actin cytoskeleton, especially through PtdIns(4,5)P_2 [41,42], and a number of the identified protein interactors are also associated with the functioning of the actin cytoskeleton. AnnexinA2 (Anxa2), which appears to bind more strongly to oxidized PTEN-GST, is a previously identified PTEN interactor [17], and it has been shown that PTEN co-localizes on the apical surface of polarized cells along with Anxa2 and the small GTPase Cdc42, which plays a role in regulating epithelial morphogenesis [43]. The authors also showed that Anxa2 binds PtdIns(4,5)P_2 at the apical surface, and noted the potential involvement of PTEN in the depletion of PtdIns(4,5)P_2 from PtdIns(3,4,5)P_3. The exact molecular mechanism responsible for the PTEN/PtdIns(4,5)P_2/Anxa2 network is still unclear, but may involve a direct association between Anxa2 and PTEN in the apical domain for the recruitment of PtdIns(4,5)P_2 to the apical surface. Another actin-binding protein, drebrin (Dreb), for which the interaction with PTEN has previously been observed in neurons [44], was also found more highly associated with oxidized PTEN-GST. PTEN has been proposed as a negative regulator of the phosphorylation of Dreb at Ser647, and the formation of the complex PTEN:Dreb seems to be inversely correlated to neuronal activity [44]. Nonetheless, a relationship between the redox status of PTEN and the molecular dynamics of the PTEN:Dreb complex has not previously been reported, and the mechanism by which PTEN binds Dreb seems to be independent of PI3K signaling. We also observed that the binding of spectrin alpha chain (non-erythrocytic 1, Spta1) to oxPTEN was significantly increased. Sptn1is involved in actin crosslinking and scaffolding to the cytoskeleton [45] helping to stabilize the plasma membrane and in the organization of intracellular organelles. Myosin phosphatase Rho-interacting protein (MPRIP), which targets myosin phosphatase to the actin cytoskeleton [46], and utrophin (Utro), which is an actin binding protein that plays an important role in the role of the cytoskeleton in the neuromuscular junction formation [47], also appeared to be interactors of PTEN that show no difference in association between oxidized or reduced PTEN-GST. PTEN has been shown to play a number of roles in neuronal cell function and development, and to localize to specific regions in neuronal cells rich in cytoskeleton, such as the growth cone and dendritic spine [48].

Another group of potentially interacting proteins are associated with DNA damage and repair, chromosomal segregation and genomic stability, and a role in DNA damage repair and response has been proposed for PTEN [49], although the knowledge of the molecular mechanism is currently limited [49]. PDIP2 (aka PDIP38) shows stronger association with oxidized PTEN, has been shown to interact with DNA polymerase delta (p50), and is involved the ability of the replication fork to pass DNA lesions, important in cell cycle control and chromosomal replication [50]. PDIP2 has also been reported to increase the activity of Nox4, a NADPH oxidase that has been identified as the main source of H_2O_2 production in non-phagocytic cells [51]. Nox4 has been shown to be activated by PtdIns(3,4,5)P_3, which triggers the increased generation of H_2O_2 resulting in the oxidation of PTEN [11]. Interestingly, our study has shown a $>$ 10-fold increase in binding of PDIP2 to the oxidized PTEN-GST, suggesting that this protein might be involved in the ROS-mediated signaling cascade responsible for PTEN inactivation. Protein pelota homolog (Pelo), which by homology to the *Drosophila* protein has been associated with chromosomal segregation during cell division and genomic stability [52], also showed significantly increased binding to oxidized PTEN. Pelo has also been shown to regulate HER2 signaling *via* the PI3K/Akt pathway [53]. PTEN has been reported to play a key role in chromosomal stability and genetic integrity through a number of interactions, including with Rad51 in the control of double-strand breaks [54], commonly caused as a result of cellular oxidative stress. DNA-damage binding protein-1 (DDB1) is a potentially novel PTEN interactor that showed no difference in binding between reduced and oxidized PTEN-GST. The interplay between the PI3K/Akt pathway and the excision nucleotide pathway, of which DDB1 is a member, has been shown in human epithelial cells [55].

Other potentially interesting novel PTEN interactors were also identified. The interactions with GNAI1/2 appeared to be significantly stronger to the oxidized protein. GNAIs are members of the Gαi family, and inhibit adenylate cyclase, playing a key role in the control of cellular proliferation and differentiation [56], processes in which PTEN also plays an important role. Fatty acid synthase (FAS) has also been linked to the Akt/PI3K pathway; a close correlation has been demonstrated between the overexpression of FAS and the loss of PTEN in HCC tissue [24], and PTEN seems to be involved in the regulation of FAS through the inhibition of Akt [57]. AKAP12 is a scaffold protein involved in the regulation of PKA and PKC in G-protein coupled receptor signaling [58]. Although the interaction of these two proteins with PTEN-GST did not appear to be redox-sensitive, they may nevertheless have an important role in metabolic regulation and cell survival.

Protein–protein interactions (PPIs) have been shown to play a major role in the biological mechanism behind many human diseases and are currently considered a promising target for the discovery and development of new drugs [59,60]. Here we provide the first report on the redox-sensitive interactome of the tumor suppressor protein PTEN. Our data showed that protein interactions with PTEN are significantly affected by its reversible oxidation, most probably the formation of the inactivating regulatory disulfide in PTEN. The *in vitro* affinity capture of proteins from cell lysates by reduced and oxidized PTEN in combination with label-free quantitative mass spectrometry has provided a valuable tool for the study of PTEN interactome under oxidative stress. We believe this method can be usefully implemented to measure the protein levels in complex biological mixtures in order to interpret MS-based proteomics datasets and has identified a new paradigm in the regulation of protein–protein interactions. The redox-alteration of the PTEN interactome is likely to play an important role in PTEN-mediated signaling, and may contribute to changes in cell function in diseases, including cancers.

Acknowledgments

This work is part of The Proxomics Project, a collaboration between Aston University, ICL and the University of Glasgow. The research presented in this paper was supported by the

Engineering and Physical Sciences Research Council (EP/I017887/1 Cross-Disciplinary Research Landscape Award). Data associated with this paper can be obtained by contacting the corresponding author.

Appendix A. Supplementary material

Supplementary data associated with this article can be found in the online version at http://dx.doi.org/10.1016/j.freeradbiomed.2015.11.004.

References

[1] J. Li, PTEN, a putative protein tyrosine phosphatase gene mutated in human brain, breast, and prostate cancer, Science 275 (1997) 1943–1947.
[2] M.P. Myers, I. Pass, I.H. Batty, J. Van der Kaay, J.P. Stolarov, B.A. Hemmings, M. H. Wigler, C.P. Downes, N.K. Tonks, The lipid phosphatase activity of PTEN is critical for its tumor suppressor function, Proc. Natl. Acad. Sci. U.S.A. 95 (1998) 13513–13518.
[3] L.C. Cantley, B.G. Neel, New insights into tumor suppression: PTEN suppresses tumor formation by restraining the phosphoinositide 3-kinase/AKT pathway, Proc. Natl. Acad. Sci. U.S.A. 96 (1999) 4240–4245.
[4] T. Tamguney, D. Stokoe, New insights into PTEN, J. Cell Sci. 120 (2007) 4071–4079.
[5] T. Maehama, J.E. Dixon, The tumor suppressor, PTEN/MMAC1, dephosphorylates the lipid second messenger, phosphatidylinositol 3,4,5-trisphosphate, J. Biol. Chem. 273 (1998) 13375–13378.
[6] E.L. Whiteman, H. Cho, M.J. Birnbaum, Role of Akt/protein kinase B in metabolism, Trends Endocrinol. Metab. 13 (2002) 444–451.
[7] D. DeFeo-Jones, S.F. Barnett, S. Fu, P.J. Hancock, K.M. Haskell, K.R. Leander, E. McAvoy, R.G. Robinson, M.E. Duggan, C.W. Lindsley, Z. Zhao, H.E. Huber, R. E. Jones, Tumor cell sensitization to apoptotic stimuli by selective inhibition of specific Akt/PKB family members, Mol. Cancer Ther. 4 (2005) 271–279.
[8] M.M. Georgescu, PTEN tumor suppressor network in PI3K-Akt pathway control, Genes Cancer 1 (2010) 1170–1177.
[9] B.A. Hemmings, D.F. Restuccia, PI3K-PKB/Akt pathway, Cold Spring Harb. Perspect. Biol. 4 (2012) a011189.
[10] S.R. Lee, K.S. Yang, J. Kwon, C. Lee, W. Jeong, S.G. Rhee, Reversible inactivation of the tumor suppressor PTEN by H_2O_2, J. Biol. Chem. 277 (2002) 20336–20342.
[11] J. Kwon, S.R. Lee, K.S. Yang, Y. Ahn, Y.J. Kim, E.R. Stadtman, S.G. Rhee, Reversible oxidation and inactivation of the tumor suppressor PTEN in cells stimulated with peptide growth factors, Proc. Natl. Acad. Sci. U.S.A. 101 (2004) 16419–16424.
[12] N.R. Leslie, D. Bennett, Y.E. Lindsay, H. Stewart, A. Gray, C.P. Downes, Redox regulation of PI 3-kinase signalling via inactivation of PTEN, EMBO J. 22 (2003) 5501–5510.
[13] K. Piotukh, D. Kosslick, J. Zimmermann, E. Krause, C. Freund, Reversible disulfide bond formation of intracellular proteins probed by NMR spectroscopy, Free Radic. Biol. Med. 43 (2007) 1263–1270.
[14] M. Tamura, J. Gu, E.H. Danen, T. Takino, S. Miyamoto, K.M. Yamada, PTEN interactions with focal adhesion kinase and suppression of the extracellular matrix-dependent phosphatidylinositol 3-kinase/Akt cell survival pathway, J. Biol. Chem. 274 (1999) 20693–20703.
[15] L. Salmena, A. Carracedo, P.P. Pandolfi, Tenets of PTEN tumor suppression, Cell 133 (2008) 403–414.
[16] O. Gorbenko, G. Panayotou, A. Zhyvoloup, D. Volkova, I. Gout, V. Filonenko, Identification of novel PTEN-binding partners: PTEN interaction with fatty acid binding protein FABP4, Mol. Cell. Biochem. 337 (2010) 299–305.
[17] J. Gunaratne, M.X. Goh, H.L. Swa, F.Y. Lee, E. Sanford, L.M. Wong, K.A. Hogue, W. P. Blackstock, K. Okumura, Protein interactions of phosphatase and tensin homologue (PTEN) and its cancer-associated G20E mutant compared by using stable isotope labeling by amino acids in cell culture-based parallel affinity purification, J. Biol. Chem. 286 (2011) 18093–18103.
[18] Y.C. Kim, H. Kitaura, T. Taira, S.M. Iguchi-Ariga, H. Ariga, Oxidation of DJ-1-dependent cell transformation through direct binding of DJ-1 to PTEN, Int. J. Oncol. 35 (2009) 1331–1341.
[19] E.J. Meuillet, D. Mahadevan, M. Berggren, A. Coon, G. Powis, Thioredoxin-1 binds to the C2 domain of PTEN inhibiting PTEN's lipid phosphatase activity and membrane binding: a mechanism for the functional loss of PTEN's tumor suppressor activity, Arch. Biochem. Biophys. 429 (2004) 123–133.
[20] J. Cao, J. Schulte, A. Knight, N.R. Leslie, A. Zagozdzon, R. Bronson, Y. Manevich, C. Beeson, C.A. Neumann, Prdx1 inhibits tumorigenesis via regulating PTEN/AKT activity, EMBO J. 28 (2009) 1505–1517.
[21] R. Aebersold, M. Mann, Mass spectrometry-based proteomics, Nature 422 (2003) 198–207.
[22] M. Vermeulen, N.C. Hubner, M. Mann, High confidence determination of specific protein–protein interactions using quantitative mass spectrometry, Curr. Opin. Biotechnol. 19 (2008) 331–337.
[23] T. Nakamura, Y. Oda, Mass spectrometry-based quantitative proteomics, Biotechnol. Genet. Eng. Rev. 24 (2007) 147–163.
[24] X. Zhu, X. Qin, M. Fei, W. Hou, J. Greshock, K.E. Bachman, R. Wooster, J. Kang, C. Y. Qin, Combined phosphatase and tensin homolog (PTEN) loss and fatty acid synthase (FAS) overexpression worsens the prognosis of chinese patients with hepatocellular carcinoma, Int. J. Mol. Sci. 13 (2012) 9980–9991.
[25] S. Nahnsen, C. Bielow, K. Reinert, O. Kohlbacher, Tools for label-free peptide quantification, Mol. Cell. Proteomics 12 (2013) 549–556.
[26] C. Kumar, M. Mann, Bioinformatics analysis of mass spectrometry-based proteomics data sets, FEBS Lett. 583 (2009) 1703–1712.
[27] M.B. Tierno, P.A. Johnston, C. Foster, J.J. Skoko, S.N. Shinde, T.Y. Shun, J.S. Lazo, Development and optimization of high-throughput in vitro protein phosphatase screening assays, Nat. Protoc. 2 (2007) 1134–1144.
[28] D.N. Perkins, D.J. Pappin, D.M. Creasy, J.S. Cottrell, Probability-based protein identification by searching sequence databases using mass spectrometry data, Electrophoresis 20 (1999) 3551–3567.
[29] D.K. Crockett, G.C. Fillmore, K.S. Elenitoba-Johnson, M.S. Lim, Analysis of phosphatase and tensin homolog tumor suppressor interacting proteins by in vitro and in silico proteomics, Proteomics 5 (2005) 1250–1262.
[30] Y. Ahn, C.Y. Hwang, S.R. Lee, K.S. Kwon, C. Lee, The tumour suppressor PTEN mediates a negative regulation of the E3 ubiquitin-protein ligase Nedd4, Biochem. J. 412 (2008) 331–338.
[31] H.J. Forman, Use and abuse of exogenous H_2O_2 in studies of signal transduction, Free Radic. Biol. Med. 42 (2007) 926–932.
[32] C. Lee, J.S. Kim, T. Waldman, PTEN gene targeting reveals a radiation-induced size checkpoint in human cancer cells, Cancer Res. 64 (2004) 6906–6914.
[33] J.S. Kim, X. Xu, H. Li, D. Solomon, W.S. Lane, T. Jin, T. Waldman, Mechanistic analysis of a DNA damage-induced, PTEN-dependent size checkpoint in human cells, Mol. Cell. Biol. 31 (2011) 2756–2771.
[34] J.P. Brennan, R. Wait, S. Begum, J.R. Bell, M.J. Dunn, P. Eaton, Detection and mapping of widespread intermolecular protein disulfide formation during cardiac oxidative stress using proteomics with diagonal electrophoresis, J. Biol. Chem. 279 (2004) 41352–41360.
[35] M.I. Berggren, B. Husbeck, B. Samulitis, A.F. Baker, A. Gallegos, G. Powis, Thioredoxin peroxidase-1 (peroxiredoxin-1) is increased in thioredoxin-1 transfected cells and results in enhanced protection against apoptosis caused by hydrogen peroxide but not by other agents including dexamethasone, etoposide, and doxorubicin, Arch. Biochem. Biophys. 392 (2001) 103–109.
[36] C.A. Neumann, J. Cao, Y. Manevich, Peroxiredoxin 1 and its role in cell signaling, Cell Cycle 8 (2009) 4072–4078.
[37] U. Schwertassek, A. Haque, N. Krishnan, R. Greiner, L. Weingarten, T.P. Dick, N. K. Tonks, Reactivation of oxidized PTP1B and PTEN by thioredoxin 1, FEBS J. 281 (2014) 3545–3558.
[38] C.M. Cruz, A. Rinna, H.J. Forman, A.L. Ventura, P.M. Persechini, D.M. Ojcius, ATP activates a reactive oxygen species-dependent oxidative stress response and secretion of proinflammatory cytokines in macrophages, J. Biol. Chem. 282 (2007) 2871–2879.
[39] S. Lu, S.B. Fan, B. Yang, Y.X. Li, J.M. Meng, L. Wu, P. Li, K. Zhang, M.J. Zhang, Y. Fu, J. Luo, R.X. Sun, S.M. He, M.Q. Dong, Mapping native disulfide bonds at a proteome scale, Nat. Methods 12 (2015) 329–331.
[40] P. Checconi, S. Salzano, L. Bowler, L. Mullen, M. Mengozzi, E.M. Hanschmann, C.H. Lillig, R. Sgarbanti, S. Panella, L. Nencioni, A.T. Palamara, P. Ghezzi, Redox proteomics of the inflammatory secretome identifies a common set of redoxins and other glutathionylated proteins released in inflammation, influenza virus infection and oxidative stress, PLoS One 10 (2015) e0127086.
[41] J.L. Li, E.J. Tanhehco, B. Russell, Actin dynamics is rapidly regulated by the PTEN and PIP2 signaling pathways leading to myocyte hypertrophy, Am. J. Physiol. – Heart Circ. 307 (2014) H1618–H1625.
[42] V. Kolsch, P.G. Charest, R.A. Firtel, The regulation of cell motility and chemotaxis by phospholipid signaling, J. Cell. Sci. 121 (2008) 551–559.
[43] F. Martin-Belmonte, A. Gassama, A. Datta, W. Yu, U. Rescher, V. Gerke, K. Mostov, PTEN-mediated apical segregation of phosphoinositides controls epithelial morphogenesis through Cdc42, Cell 128 (2007) 383–397.
[44] P. Kreis, R. Hendricusdottir, L. Kay, I.E. Papageorgiou, M. van Diepen, T. Mack, J. Ryves, A. Harwood, N.R. Leslie, O. Kann, M. Parsons, B.J. Eickholt, Phosphorylation of the actin binding protein Drebrin at S647 is regulated by neuronal activity and PTEN, PLoS One 8 (2013) e71957.
[45] A. Chakrabarti, D.A. Kelkar, A. Chattopadhyay, Spectrin organization and dynamics: new insights, Biosci. Rep. 26 (2006) 369–386.
[46] H.K. Surks, C.T. Richards, M.E. Mendelsohn, Myosin phosphatase-Rho interacting protein – a new member of the myosin phosphatase complex that directly binds RhoA, J. Biol. Chem. 278 (2003) 51484–51493.
[47] G.C. Dobbins, B. Zhang, W.C. Xiong, L. Mei, The role of the cytoskeleton in neuromuscular junction formation, J. Mol. Neurosci. 30 (2006) 115–118.
[48] P. Kreis, G. Leondaritis, I. Lieberam, B.J. Eickholt, Subcellular targeting and dynamic regulation of PTEN: implications for neuronal cells and neurological disorders, Front. Mol. Neurosci. 7 (2014) 23.
[49] M. Ming, Y.Y. He, PTEN in DNA damage repair, Cancer Lett. 319 (2012) 125–129.
[50] L. Liu, E.M. Rodriguez-Belmonte, N. Mazloum, B. Xie, M.Y.W.T. Lee, Identification of a novel protein, PDIP38, that interacts with the p50 subunit of DNA polymerase delta and proliferating cell nuclear antigen, J. Biol. Chem. 278 (2003) 10041–10047.
[51] F.J. Miller Jr., NADPH oxidase 4: walking the walk with Poldip2, Circ. Res. 105 (2009) 209–210.
[52] R. Shamsadin, I.M. Adham, G. von Beust, W. Engel, Molecular cloning,

expression and chromosome location of the human pelota gene PELO, Cytogenet. Cell Genet. 90 (2000) 75–78.
[53] K. Pedersen, F. Canals, A. Prat, J. Tabernero, J. Arribas, PELO negatively regulates HER receptor signalling and metastasis, Oncogene 33 (2014) 1190–1197.
[54] W.H. Shen, A.S. Balajee, J. Wang, H. Wu, C. Eng, P.P. Pandolfi, Y. Yin, Essential role for nuclear PTEN in maintaining chromosomal integrity, Cell 128 (2007) 157–170.
[55] Y.R. Chen, M.T. Liu, Y.T. Chang, C.C. Wu, C.Y. Hu, J.Y. Chen, Epstein-Barr virus latent membrane protein 1 represses DNA repair through the PI3K/Akt/FOXO3a pathway in human epithelial cells, J. Virol. 82 (2008) 8124–8137.
[56] J. Yao, L.H. Liang, Y. Zhang, J. Ding, Q. Tian, J.J. Li, X.H. He, GNAI1 suppresses tumor cell migration and invasion and is post-transcriptionally regulated by Mir-320a/c/d in hepatocellular carcinoma, Cancer Biol. Med. 9 (2012) 234–241.
[57] T. Van de Sande, E. De Schrijver, W. Heyns, G. Verhoeven, J.V. Swinnen, Role of the phosphatidylinositol 3'-kinase/PTEN/Akt kinase pathway in the overexpression of fatty acid synthase in LNCaP prostate cancer cells, Cancer Res. 62 (2002) 642–646.
[58] M.H. Chen, C.C. Malbon, G-protein-coupled receptor-associated A-kinase anchoring proteins AKAP5 and AKAP12: differential trafficking and distribution, Cell Signal. 21 (2009) 136–142.
[59] A.I. Archakov, V.M. Govorun, A.V. Dubanov, Y.D. Ivanov, A.V. Veselovsky, P. Lewi, P. Janssen, Protein–protein interactions as a target for drugs in proteomics, Proteomics 3 (2003) 380–391.
[60] D.P. Ryan, J.M. Matthews, Protein–protein interactions in human disease, Curr. Opin. Struct. Biol. 15 (2005) 441–446.